Can coseismic stress variability suppress seismicity shadows? Insights from a rate-and-state friction model

D. Marsan[1]

Received 20 September 2005; revised 16 December 2005; accepted 16 February 2006; published 15 June 2006.

[1] The paucity of detectable seismicity shadows in the days/months following a main shock has raised the question as to whether dynamic rather than static triggering could be the main mechanism driving the seismicity at these timescales. The lack of correlation between the stress unloading of the main fault and the typically vigourous aftershock production taking place on it, however, suggests that the spatial heterogeneity of the coseismic stress change could also be a factor in the apparent suppression of seismicity shadows, at least on the main fault. Here we study whether this stress variability can indeed be an important aspect in the stress modeling of earthquake sequences. A rate-and-state friction model of seismicity is used, in conjunction with realistic levels of stress heterogeneity at the earthquake nucleation scale (1–10 m, as predicted from these friction laws), based on scale-invariant models of coseismic slip distribution. In this model, a relatively weak on-fault quiescence is delayed by months to years because of the high stress heterogeneity. Delayed quiescences due to slip heterogeneity are similarly predicted at distances of up to about half the rupture length away from the fault. We also postulate that off-fault seismicity can be significantly controlled by stress variability that originates from small-scale crustal heterogeneity and the complexity in fault geometries. Rather than mapping stress changes by providing a single stress value at every grid point, these results suggest that an estimate of the likely stress variability (acting at the nucleation scale) is also needed, especially when trying to account for the seismicity occurring at relatively short timescales.

Citation: Marsan, D. (2006), Can coseismic stress variability suppress seismicity shadows? Insights from a rate-and-state friction model, *J. Geophys. Res.*, *111*, B06305, doi:10.1029/2005JB004060.

1. Introduction

[2] Aftershock triggering is an ubiquitous feature of earthquake sequences. The mean stress drop on a fault that has experienced an earthquake typically ranges between 0.1 to 50 MPa [*Hanks*, 1977; *Abercrombie and Leary*, 1993]. That such a sudden decrease in shear stress systematically leads to an increase of on-fault seismicity is a clear indication that this relaxation is far from being uniform: the surface averaged stress change is negative, but parts of the fault must have undergone an increase in shear stress. This has been observed by *Mikumo and Miyatake* [1995], *Bouchon* [1997], *Bouchon et al.* [1998], *Day et al.* [1998], *Dalguer et al.* [2002], *Zhang et al.* [2003], and *Ripperger and Mai* [2004] for a number of earthquakes.

[3] On the main fault, the mean decrease of the stress should imply that, following an initial aftershock sequence caused by the nonuniformity of the stress drop, a quiescence eventually develops. While seismicity shadows have been found to be less frequently observed at short timescales (e.g., months) than what static Coulomb modeling would predict [*Parsons*, 2002; *Marsan*, 2003; *Marsan and Nalbant*, 2005; *Felzer and Brodsky*, 2005], they appear to emerge much more clearly at timescales of years to tens of years after a large earthquake. For example, the 1857 Fort Tejon earthquake has been found by *Harris and Simpson* [1996] to produce a shadow lasting for at least 50 years, in the sense that the known earthquake activity in southern California mostly occurred in locations that experienced positive Coulomb stress changes. This long-term absence of earthquakes in the unloaded areas followed an initial 3.75 years, at least, of aftershock activity as proposed by *Meltzner and Wald* [1999]. Seismicity following the 1906 San Francisco earthquake has been shown to exhibit the same type of behavior [*Ellsworth et al.*, 1981; *Harris and Simpson*, 1998; *Meltzner and Wald*, 2003]. Analysis of the aftershock sequence of the 1999 Chi-Chi earthquake, Taiwan, by *Ma et al.* [2005] has shown that indeed triggering is first observed in areas that are expected to be stress shadows, lasting for about 3 months and hence in agreement with the 100 day timescale of *Marsan* [2003] obtained for the 1992 Landers and the 1994 Northridge earthquakes. Quiescence can eventually be obtained for

[1]Laboratoire de Géophysique Interne et Tectonophysique, Université de Savoie, Le Bourget du Lac, France.

Copyright 2006 by the American Geophysical Union.
0148-0227/06/2005JB004060$09.00

these zones, at longer timescales. At such timescales, it can, however, become difficult to causally relate a change in seismicity (be it triggering or quiescence) to the occurrence of the main shock. For example, *Ogata et al.* [2003] attributed a decrease in activity starting 6 months after the 1992 Landers earthquake to a different origin than the main shock itself. Similarly, a clear quiescence following initial triggering is found at the Yalova swarm, Turkey, following the 1999 Düzce earthquake; this quiescence was apparently not caused by a seismic event [*Daniel et al.*, 2006].

[4] In statistical terms, the two phases of initial aftershock triggering and longer term quiescences on the main fault can therefore be expected to be controlled by (1) the variance and (2) the mean of the coseismic stress change, respectively. For earthquake occurrence, these two characteristics of the on-fault coseismic stress change are thus operating at different time scales.

[5] Many models have been invoked to explain aftershock generation. It has been proposed that transient stress changes can also drive this phenomenon [*Gomberg et al.*, 1998, 2003; *Kilb et al.*, 2000, 2002; *Voisin et al.*, 2000, 2004; *Felzer and Brodksy*, 2005; *Parsons*, 2005]. While the dynamic stress becomes rapidly much greater than the static one as one moves away from the main shock, we here consider the specific case of on-fault seismicity, for which both stresses are expected to be of the same order. Evidence for on-fault triggering by dynamical stress has, however, been proposed by *Gomberg et al.* [2003]. Also, it is still an open question as to whether a perturbation lasting several tens of seconds can cause earthquake occurrence months to years later [*Belardinelli et al.*, 2003; *Parsons*, 2005]. Another model explains aftershock decaying rates by stress transfer from a velocity-strengthening deep layer, therefore expecting that both afterslip and aftershock occurrences decay at the same rate [*Perfettini and Avouac*, 2004]. Such a mechanism would, however, predict a very significant increase of seismicity with depth, as the reloading is made from deeper parts of the fault.

[6] This present contribution is a study of how rate-and-state friction modeling can reproduce the two features of initial aftershock triggering followed by long-lasting quiescence on the main fault. The two fundamental working hypotheses are that static stress drop variability matters when considering the temporal evolution of on-fault seismicity, and that one can realistically relates static stress changes to seismicity changes using rate-and-state friction.

2. Rate-and-State Friction Modeling

[7] This treatment follows the approach of *Dieterich* [1994]: the quasi-static motion of a great number of fault patches accelerating toward failure is modelled, by considering a rate-and-state friction [*Dieterich*, 1979; *Ruina*, 1983] opposing the tectonic forcing stress. The time evolution of the state variable follows the slowness law [*Dieterich*, 1986].

[8] Within this framework, the seismicity rate $\lambda(t)$ evolves as $\lambda = \frac{\mu}{\gamma\dot{\tau}}$ with μ the stationary background rate, $\dot{\tau}$ the tectonic stress loading rate, and γ a function such that $d\gamma = dt - \gamma d\tau$. Here τ is a quantity uniformly increasing with time $d\tau/dt = \dot{\tau}$, to which stress steps $\{\tau_i\}$ occurring at times $\{t_i\}$ are added. All stresses are in units of $A\sigma$, where A is a constitutive parameter of rate-and-state friction, and σ is the normal stress acting on the fault. All times are in units of $t_a = \frac{A\sigma}{\dot{\tau}}$, which is thought to represent the typical duration of an aftershock sequence (see section 2.2 for a slightly different perspective on this). Several assumptions are made in the following treatment:

[9] 1. There are no changes in normal stress σ, as expected for a planar fault, and σ is also uniform over the fault. Changes in normal stress can be accounted for by replacing the shear stress τ by a Coulomb stress $\tau - \mu_f\sigma$ [see *Perfettini et al.*, 2003]. A nonuniform, or even a strongly heterogeneous σ, would enhance the overall stress variability, hence the assumption of uniformity is a conservative one in this study.

[10] 2. The inertial terms in the equations describing the motion of the fault are neglected, so that any given portion of the fault is in mechanical equilibrium at all times.

[11] 3. The changes in stress are permanent (i.e., static stress) and are applied suddenly (i.e., no dynamical stresses).

[12] 4. Poroelasticity and viscoelasticity effects are not considered.

2.1. Seismicity Rate Changes

[13] For a fault initially at steady state, and undergoing the N stress changes $\{\tau_i\} = \tau_1, \ldots, \tau_N$ at times $\{t_i\}$, the function γ is

$$\gamma(t < t_1) = \frac{1}{\dot{\tau}}$$

$$\gamma(t_1 < t < t_2) = \frac{1}{\dot{\tau}} \times \left\{1 + e^{-(t-t_1)}(e^{-\tau_1} - 1)\right\}$$

$$\gamma(t_2 < t < t_3) = \frac{1}{\dot{\tau}} \times \left\{1 + e^{-(t-t_1)} \times (e^{-\tau_1-\tau_2} - e^{-\tau_2} + e^{t_2-t_1}(e^{-\tau_2} - 1))\right\} \ldots$$

[14] This can be rewritten as

$$\gamma(t_i < t < t_{i+1}) = \frac{1}{\dot{\tau}} \times \left\{1 + e^{-(t-t_1)}\,\epsilon_i\right\} \tag{1}$$

with the factor ϵ_i obtained in a recursive manner:

$$\epsilon_i = \epsilon_{i-1}\, e^{-\tau_i} + e^{t_i-t_1}(e^{-\tau_i} - 1) \tag{2}$$

starting at $t < t_1$ with $\epsilon_0 = 0$. Note that $\epsilon_i \times e^{-(t_i-t_1)} > -1$, with large values of ϵ obtained after strong stress decreases $\tau \ll -1$ and low values after strong stress increases $\tau \gg 1$. This yields a seismicity rate $\lambda(t_i < t < t_{i+1}) = \mu/[1 + e^{-(t-t_i)}\epsilon_i]$. Denoting by Λ_1 the extra seismicity due to τ_1 acting on its own (i.e., number of earthquakes caused by the triggers in the case $N = 1$ of only one trigger), we get that

$$\begin{aligned}\Lambda_1 &= \int_{t_1}^{\infty} dt\ (\lambda - \mu) \\ &= \left[\mu \ln\left(1 + \epsilon_1\, e^{-(t-t_1)}\right)\right]_{t_1}^{\infty} \\ &= \mu\tau_1\end{aligned} \tag{3}$$

i.e., the number of triggered earthquakes is proportional to the shear stress change τ_1. In the general case of N stress changes $\{\tau_i\}$, this becomes

$$\Lambda_{1,\ldots,N} = \int_{t_1}^{\infty} dt\ (\lambda - \mu) = \sum_{i=1}^{N} \int_{t_i}^{t_{i+1}} dt \left(\frac{\mu}{1 + \epsilon_i e^{-(t-t_1)}} - \mu \right) \quad (4)$$

with $t_{N+1} = \infty$, which finally yields

$$\Lambda_{1,\ldots,N} = \mu(\tau_1 + \tau_2 + .. + \tau_N) = \Lambda_1 + \Lambda_2 + .. + \Lambda_N \quad (5)$$

[15] The model is therefore linear in terms of the total seismicity changes caused by a set of triggers, although it is not when considering finite timescales. Also, $\Lambda_{1,\ldots,N}$ does not depend on the exact stress history of the trigger sequence, though the time-dependent rate $\lambda(t)$ obviously does.

2.2. On-Fault Seismicity

[16] We now consider the case of on-fault seismicity triggered after a main shock. As a first approximation, it is assumed that only the main shock triggers seismicity. The case of multiple interactions between aftershocks will be studied in section 2.3. A first observation is that, in the framework of rate-and-state friction, since the ratio of the total number of aftershocks to the background rate Λ/μ equals the average stress drop $\overline{\tau}$, this number should be negative: overall, the seismicity is expected to decrease following an earthquake. As is discussed in this section, this only occurs at long timescales.

[17] We model the spatial variability of the coseismic stress drop τ as a Gaussian distribution with mean $\overline{\tau} < 0$ (i.e., a decrease of shear stress on surface average) and standard deviation σ_τ. We denote by λ the seismicity change for a local patch of the fault for which the stress change is uniform, and λ_{fault} the overall seismicity change for the whole fault:

$$\lambda_{\text{fault}}(t) = \int d\tau\ \frac{1}{\sqrt{2\pi}\sigma_\tau} e^{-(\tau-\overline{\tau})^2/2\sigma_\tau^2}\ \frac{\mu}{1 + e^{-t}(e^{-\tau} - 1)} \quad (6)$$

It can then be shown that the following occur:

[18] 1. At $t = 0^+$ immediately after the main shock, the response of the fault to the stress change is strongly asymmetrical in favor of triggering: $\lambda(t = 0^+) = \mu e^{\tau}$; hence

$$\lambda_{\text{fault}}(t = 0^+) = \int d\tau\ \frac{1}{\sqrt{2\pi}\sigma_\tau} e^{-(\tau-\overline{\tau})^2/2\sigma_\tau^2}\ \mu e^{\tau} = \mu e^{\overline{\tau} + \sigma_\tau^2/2} \quad (7)$$

For a low variability, $\sigma_\tau < \sqrt{2|\overline{\tau}|}$ immediate quiescence is obtained (since $\overline{\tau} < 0$), while high variability $\sigma_\tau > \sqrt{2|\overline{\tau}|}$ will promote initial triggering, tending to $\lambda_{\text{fault}}(t = 0^+) \simeq \mu e^{\sigma_\tau^2/2}$ as σ_τ increases.

[19] 2. At long timescales, λ_{fault} must be less than μ in order to ensure that the total number of triggered earthquakes is negative $\int_0^{\infty} dt\ \lambda_{\text{fault}}(t) = \Lambda_1 = \mu\overline{\tau}$ as shown in section 2.1.

[20] The evolution of λ_{fault} with time can be studied numerically and is shown in Figure 1 for varying values of σ_τ. Here we take $\overline{\tau} = -100$, which is a typical ratio of stress drop (1–10 MPa) to $A\sigma$ (0.01–0.1 MPa [see, e.g., *Toda et al.*, 1998]). The existence of a triggering phase here requires that $\sigma_\tau > 14.2$. Quiescence is seen to occur in all cases, with an early Omori decay for $\sigma_\tau > 30$ only. As σ_τ increases, the quiescence starts later but lasts longer. Its "intensity" (defined as the maximum departure from the background seismicity rate) decays with σ_τ. Dependence on σ_τ of the starting and ending times (the latter is here defined as the time when $\lambda/\mu = 0.99$) of the quiescence, along with the minimum rate ratio λ/μ, is summarized in Figure 2. Strong quiescence, with min $\lambda/\mu \ll 0.1$, starting shortly after the main shock at $t \simeq 10^{-2}$, is obtained for relatively low σ_τ, i.e., of the order of 50 to 80, hence less than $|\overline{\tau}|$. In comparison, larger values of σ_τ lead to much longer shadows that start much later but that are weaker, only reducing the background seismicity rate by 50%. At large values of $|\overline{\tau}|$ and σ_τ, it can be shown that the start t_s of the quiescence is well approximated by $t_s = -\ln(\frac{1}{2} + \frac{1}{2}\text{erf}(-\overline{\tau}/\sqrt{2}\sigma_\tau))$; hence t_s only depends on the ratio $\sigma_\tau/\overline{\tau}$. As already mentioned, the aftershock phase can last significantly less than 1 in the case of little disorder. This can perhaps have some consequences when directly estimating t_a from the observed duration of a sequence. The power law decay $\lambda_{\text{fault}} \sim t^{-p}$ of the rate in the triggering phase yields p values typically less than 1, as observed on Figure 1. Using an exponential fall-off of the stress distribution, with mean and standard deviation equal to σ_τ, A. Helmstetter and B. E. Shaw (Estimating stress heterogeneity from aftershock rate, submitted to *Journal of Geophysical Research*, 2005, hereinafter referred to as Helmstetter and Shaw, submitted manuscript, 2005) have shown that $p = 1 - \frac{1}{\sigma_\tau}$, hence $p \to 1$ when $\sigma_\tau \to \infty$.

[21] A good approximation that lends itself to simple analytical treatment is given by a binary distribution of τ: $\tau = \overline{\tau} \pm \sigma_\tau$ with equal probability, hence keeping $\overline{\tau}$ and σ_τ as the mean and standard deviation of τ, respectively. In the case of high coseismic stress variability $\sigma_\tau \gg \sqrt{|\overline{\tau}|}$, two regimes are found. Initial triggering decays as $1/t$ until $t = \ln 2 \simeq 0.69$, at which time $\lambda_{\text{fault}} = \mu$. This time of ln 2 is found in Figure 2 as a limit when $\sigma_\tau \to \infty$. This is then followed by long-term quiescence, with a characteristic ending time proportional to σ_τ, i.e., $\lim_{t\to\infty}\lambda_{\text{fault}} = \mu - e^{\sigma_\tau} e^{-t}$ so that λ_{fault} tends asymptotically to μ as $t \to \infty$. This regime has a minimum seismicity rate value $\lambda_{\text{fault}} = \mu/2$ independent of σ_τ, obtained at $t = \sigma_\tau/2$ (see also Figure 2, where this rate change of 1/2 is obtained in the limit $\sigma_\tau \to \infty$).

[22] These observations have strong implications for the evolution of seismicity during the earthquake cycle, as the variability σ_τ of the coseismic stress drop not only controls the intensity of the aftershock regime, but also, and more unexpectedly, the duration of the following quiescence that can develop years after this variability was coseismically generated.

2.3. Multiple Interactions

[23] It has been hypothesized so far that only the stress changes caused by the main shock could act on the seismicity rate. It has, however, been suggested [*Felzer et*

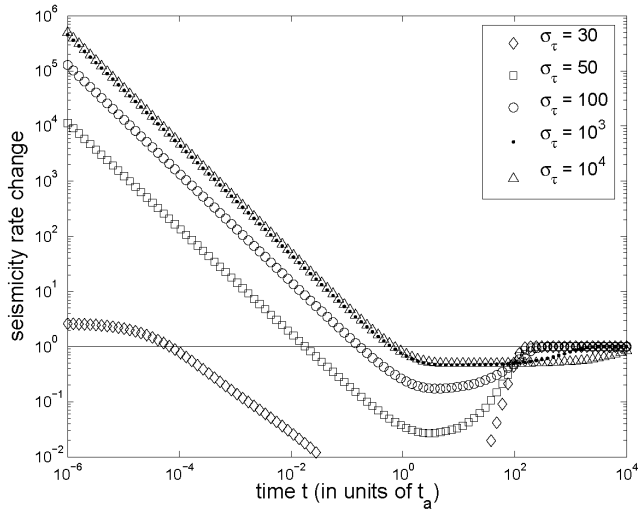


Figure 1. Seismicity rate change λ/μ versus time t in units of t_a, for a stress drop with mean $\overline{\tau} = -100$ and varying standard deviation σ_τ. The stress drop is in units of $A\sigma$. Quiescence is observed to emerge after an initial triggering phase.

al., 2002, 2004; *Helmstetter*, 2003; *Helmstetter et al.*, 2005; *Marsan*, 2005] that small earthquakes, and hence aftershocks, can play a significant role in triggering other small (or larger) earthquakes. Clustering of the hypocenters implies that the stress generated by large numbers of small shocks at the nucleation sites of future earthquakes is not negligible. Analysis of the spatial relation between microruptures on creeping faults in California has shown that these ruptures clearly influence each other [*Rubin and Gillard*, 2000] (see also *Fischer and Horálek* [2005] for similar conclusions obtained for a strike-slip swarm in West Bohemia), leading to clustering. This somewhat contrasts with the conclusions of *Ziv and Rubin* [2003], who reported that including multiple interactions does not alter the response of a fault to a stress step, as modeled by quasi-static rate-and-state friction. *Ziv and Rubin* [2003, Figure 6], however, show clear quiescence phases emerging at times of the order of 0.1 to 1 (still in units of t_a), with intensities increasing with the magnitude of the stress step. Some of this quiescence can probably be attributed to the finite population of cells, since a recently broken cell will first need to be reloaded before again accelerating to failure. The question as to the influence of the number of cells in this model on the existence and timing of such a quiescence can therefore be asked. Indeed, *Gomberg et al.* [2005] found that quiescence can arise from finite fault population models, the timing depending on the number of cells. While rate-and-state friction predicts the existence of a minimum scale for slip instability to occur, it is difficult to use this length for realistically estimating such a number; fault roughness, the existence of a damage zone surrounding the fault core, hence of a nonplanar but rather a volumic, possibly fractal, "fault," and the choice of how long an "isolated" fault can be, if this has a meaning at all, will certainly influence this number.

[24] We here examine how multiple interactions during the aftershock sequence can modify the pattern described in section 2.2 but for an infinitely large number of sources: each fault patch is allowed to fail successively, the timing of which being constrained by the evolution of the seismicity rate governed by rate-and-state friction. Knowing that N earthquakes have occurred at times $\{t_i\}$, and have exerted shear stress changes $\{\tau_i\}$ on a given fault segment, the time of occurrence $t_N + \delta t$ of the next earthquake on this given segment can be calculated. This assumes that, apart from the tectonic loading at constant stress rate $\dot{\tau}$, no further stress change is experienced by the fault during the time interval δt. The integral between t_i and $t_i + \delta t$ of the seismicity rate $\lambda(t)$ is given by

$$\int_{t_i}^{t_i+\delta t} dt\ \lambda(t) \;=\; \mu\ \delta t + \mu \ln\left(1 - \frac{\epsilon_i\ e^{-(t_i - t_1)}}{1 + \epsilon_i\ e^{-(t_i - t_1)}}\ \left(1 - e^{-\delta t}\right)\right) \tag{8}$$

We use equation (8) to model multiple interactions between earthquakes triggered after the main shock. Namely, this Markovian model applies the following algorithm:

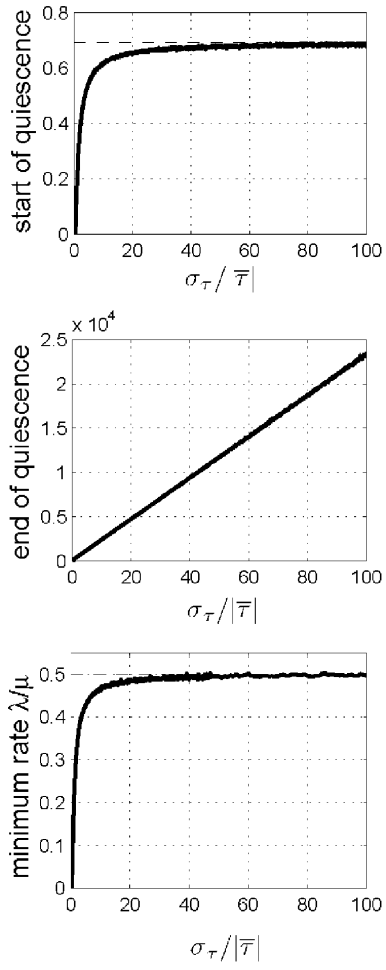


Figure 2. (top) Starting time, (middle) ending time, and (bottom) minimum rate of the quiescence period, for $\overline{\tau} = -100$, versus σ_τ. The ending time is defined as the time when $\lambda/\mu = 0.99$. The starting time tends to log 2 (dashed line). The minimum rate tends to 0.5 (dashed line).

[25] 1. At $t_1 = 0$, occurrence of the main shock creates a shear stress change modeled as an instance of a Gaussian white noise, with mean $\overline{\tau}$ and standard deviation σ_τ. N independent samples $\{\tau_j\}$ of this law are drawn. Index i is set to 1.

[26] 2. For each sample j, the factor ϵ_i defined in equation (2) is computed.

[27] 3. The new seismicity rate at $t > t_i$ and before the occurrence of the next earthquake is

$$\lambda(t) \;=\; E\left\{\frac{\mu}{1+\epsilon_i\, e^{-(t-t_1)}}\right\} \tag{9}$$

where the average is taken over the N samples. The waiting time δt until the next earthquake at $t_{i+1} = t_i + \delta t$ is therefore obtained by numerically solving the equation

$$\mu\,\delta t \;+\mu\, E\left\{\ln\left(1-\frac{\epsilon_i\, e^{-(t_i-t_1)}}{1+\epsilon_i\, e^{-(t_i-t_1)}}\left(1-e^{-\delta t}\right)\right)\right\} = \;-\ln U \tag{10}$$

where U is a uniform random variable between 0 and 1.

[28] 4. The change in shear stress τ caused by this new earthquake is modeled as a Gaussian random variable of zero mean and standard deviation σ'_τ. Index i is incremented by 1, and the procedure starts again from step 2.

[29] This model can be seen as the simplest one that accounts for multiple interactions, even though it admittedly is too simple to be realistic. The two important ingredients are (1) that the occurrence of an aftershock further roughen the stress field, by adding variability to it and (2) that a mean stress change equal to zero for all the aftershocks implies that any observed seismicity shadow is only due to the main shock (section 2.1). The first ingredient creates a feedback loop in the seismogenic process, of the form aftershocks $\rightarrow$ extra stress disorder $\rightarrow$ extra triggering $\rightarrow$ aftershocks. The aftershocks are thus merely seen as events that create further stress disorder. They all have the same "size," since the added disorder is statistically the same for all of them. A constant size is assumed to stabilize the model, especially as an ensemble-averaged behavior is studied here.

[30] Since the aftershocks do not change the long-term number of triggered earthquakes (second ingredient), their role is here only to modulate the response of the fault at finite timescales. The choice of a random white Gaussian noise field for the stress drop is only a very crude approximation of reality, as will be discussed in section 3, but one that simply generates an heterogeneous stress for each event, including the main shock. This is the minimum requirement for studying how such heterogeneity can influence the evolution of the seismicity rate through multiple interactions.

[31] This model does not distinguish a "locked" phase from an "accelerating" phase as done by *Dieterich* [1995] and *Ziv and Rubin* [2003]. The clock advance Δt of a fault patch which at time t from failure experiences a stress change τ is $\Delta t = \ln[e^{-t} + e^{-\tau}(1 - e^{-t})]$ [*Gomberg et al.*, 1998] for accelerating patches, i.e., such that slip speed is much greater than D_c/θ where D_c is the critical slip distance and θ the state variable entering the rate-and-state friction formulation. For $t \gg 1$, this gives $\Delta t \simeq -\tau$, which is also the clock advance of a locked patch [see also *Gomberg et al.*, 2005]. Early in the acceleration phase, a fault patch behaves the same as during the preceding locked phase in terms of clock advance, as long as the duration of the accelerating phase is greater than 1.

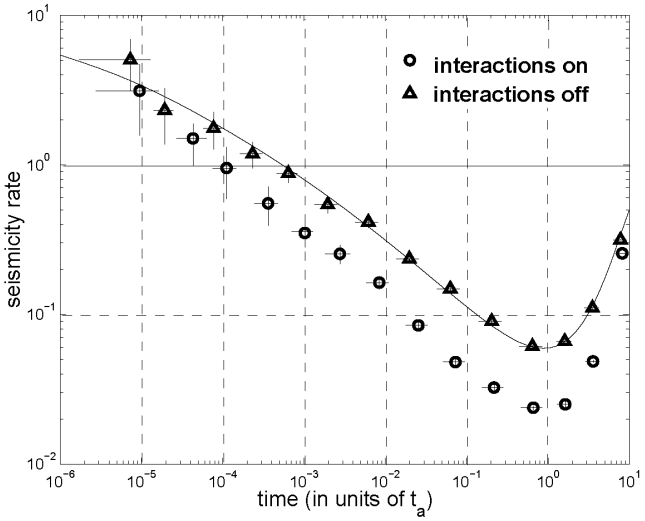


Figure 3. Seismicity rate change $\lambda(t)$ divided by steady state rate, in the cases of triggering by the main shock only (triangles) and of multiple interactions (circles), for $\overline{\tau} = -10$, $\sigma_\tau = 4$, and $\sigma'_\tau = 0.1$. The steady state rate is μ in the first case, and about $1.22 \times \mu$ in the second case. The seismicity rate changes are computed by ensemble averaging over different runs of the model: the standard deviation of $\lambda(t)$ shown by the error bars is estimated as $1/\delta t \times \sqrt{n(1-n/N)}$, where δt is the size of the time bin, n is the number of earthquakes occurring in this bin, and N is the total number of earthquakes. The case of no interactions follows the rate change in continuous line predicted by equation (6).

[32] Preconditioning of the model is required, so that a stationary regime is reached by the fault before the occurrence of the main shock.

[33] This model was run for the two sets of values: $\overline{\tau} = -10$, $\sigma_\tau = 4$ and 10, and $\sigma'_\tau = 0.1$. In each case, several tens of simulations were run, to yield an average seismicity rate. For a model with no main shock, hence only small events ("aftershocks") triggering each other, the seismicity rate was observed to be constant following a transient regime. This steady state rate is found to be larger than μ, depending on the choice of σ'_τ; for $\sigma'_\tau = 0.1$, this rate is about 1.22 times μ. The disorder created by the small shocks therefore promote temporal clustering of the events, and in the stationary regime this amounts to an increase in the mean rate. When the main shock is forced to occur (after the system has settled down to its steady state regime), strong triggering is observed, but the ratio of the aftershock rate to the steady state rate is less than the ratio of the aftershock rate to μ in the case of no multiple interactions, compare Figures 3 and 4. While the existence of an initial triggering phase followed by long-term quiescence is again verified, the latter is found to start in

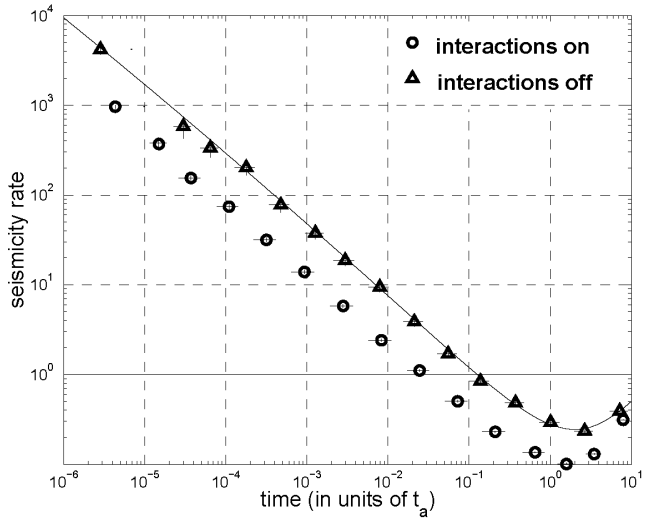


Figure 4. Same as in Figure 3 but for $\sigma_\tau = 10$.

advance compared to the case of triggering by the main shock only.

3. How Spatially Variable Is the Stress Drop?

[34] So far, the stress drop τ was simply distributed as a Gaussian white noise with a standard deviation σ_τ that has yet to be properly constrained. Hence the question remains as to how variable the coseismic stress drop is, especially at the scales that matter for the nucleation and propagation of small ruptures. Extrapolation of inverted stress drop distributions to small scales, using scale-invariant models of slip as proposed by several authors [*Andrews*, 1980; *Frankel*, 1991; *Herrero and Bernard*, 1994; *Mai and Beroza*, 2002] suggest that its variability could grow and diverge at small spatial scales. We develop this argument for a two-dimensional scale-invariant model of slip where the slip $u(\underline{k})$ is proportional to $k^{-1-H}\gamma(\underline{k})$, with H the Hurst exponent related to the fractal dimension D by $3 = D + H$, γ a Gaussian white noise, and $\underline{k}$ the wave number. The k^{-2} model [e.g., *Herrero and Bernard*, 1994] assumes $H = 1$, hence a rather smooth slip distribution. In their extended analysis of the slip distributions of 44 earthquakes, *Mai and Beroza* [2002] found that $H = 0.71 \pm 0.23$. Since the stress drop scales as $\tau(\underline{k}) \sim k\, u(\underline{k}) \sim k^{-H}\, \gamma(\underline{k})$, the scaling of the standard deviation $\sigma_\tau(\ell)$ of the stress drop τ at scale ℓ is given by

$$\sigma_\tau^2(\ell) \sim \int_{1/L}^{1/\ell} dk\; k\; |\tau(k)|^2 \Rightarrow \sigma_\tau(\ell) \sim \left[\left(\frac{L}{\ell}\right)^{2-2H} - 1\right]^{1/2} \quad (\text{for } H < 1) \tag{11}$$

$$\sim \left[\ln\frac{L}{\ell}\right]^{1/2} \quad (\text{for } H = 1) \tag{12}$$

where L is the size of the coseismic rupture. Isotropy of both the slip and stress drop is assumed. In the limit of $\ell \to 0$, $\sigma_\tau(\ell) \sim \ell^{H-1} \to \infty$. Figure 5 shows $\sigma_\tau(\ell)$ for H ranging from 0.5 to 1, as given by equations (11) and (12).

[35] To illustrate this argument, we consider the case of the 1994 M_w6.7 Northridge earthquake. Its slip distribution was found by *Mai and Beroza* [2002] to be characterized by $H = 0.68$. Taking $L = 20$ km as the representative rupture size of this event, and $\sigma_\tau(\ell = 4\text{ km}) = 4.78$ MPa [*Bouchon*, 1997], this standard deviation is found to be 8.58, 18.9, 39.8, and 83.4 MPa at the 1 km, 100 m, 10 m, and 1 m scales. The mean stress drop has been estimated to $\overline{\tau} = -2.28$ MPa [*Bouchon*, 1997]. If such an extrapolation to small scales is realistic, then very high stresses of tens to hundreds of megapascals are probable.

[36] Fractal models of slip distribution imply that stress disorder depends on scale. However, it is yet unclear as to what scale actually matters for earthquake triggering. It has been suggested by *Beroza and Ellsworth* [1996] and *Dodge et al.* [1995] that earthquakes nucleate over an area which size amounts to typically 10% of the total size of the rupture. This would imply that large earthquakes "see" a smoother stress field compared to their smaller counterparts. A very different conclusion was reached by *Lapusta and Rice* [2003], who showed that rate-and-state modeling of the nucleation and propagation of earthquakes in a crust with depth-dependent frictional properties predicts that the nucleation phase is the same for all earthquakes regardless of their sizes, large earthquakes only differing from smaller ones by the ability of their nucleating slip patch to run away and propagate the instability over long distances, as a consequence of a "favorable" stress configuration. They also propose that nucleation takes place at the 1 m to 10 m scales. As seen above, the stress drop standard deviation is likely to be very large at such small scales, typically of the

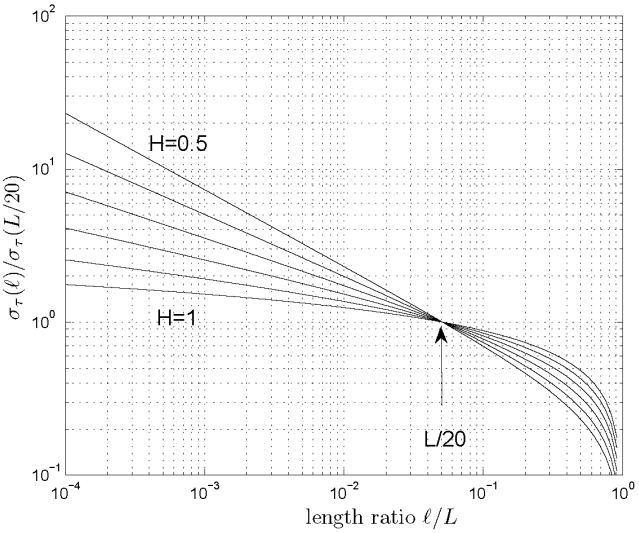


Figure 5. Increase of $\sigma_\tau(\ell)$, the stress variability (standard deviation) at scale ℓ, with the decrease of ℓ, for a fractal Gaussian slip model with varying Hurst exponent H ranging from 0.5 to 1. This graph represents the generic case of a fault of total length L, for which the stress variability is known down to scale $L/20$; such a scale is generally $\simeq$5 km, so this corresponds to a $\simeq$100 km long fault (i.e., a magnitude $\simeq$ 7.5 earthquake).

order of several tens times the mean stress drop: on-fault aftershocks would therefore nucleate over a very rough stress field.

[37] A very different type of slip distribution from the Gaussian fractal models mentioned above was proposed by *Lavallée and Archuleta* [2003, 2005] for the 1979 Imperial Valley and 1999 Chi-Chi earthquakes, which they found to follow a Lévy stable law, with stability index α_L close to 1 in both cases. Such a distribution is heavy tailed, the probability density function decaying slowly in $\tau^{-1-\alpha_L}$, implying that very large values are much more likely than as predicted by a Gaussian distribution. A standard deviation cannot be defined for $\alpha_L < 2$. The analyses by *Lavallée and Archuleta* [2003, 2005], however, suffer from the limited number of available data (i.e., number of slip values for the earthquake), and one can expect a truncated Lévy law to be more pertinent than a nontruncated one. This truncation is required to limit the possible slip values to realistic intervals, so to at the very least prevent stress values to be larger than the plastic yield stress. In any case, a (truncated) Lévy-distributed stress drop would produce a much higher variability than what is predicted by Gaussian models as described above, which only provide lower bounds for the stress drop variability.

4. Conclusions

[38] Strong and long-lasting earthquake triggering is systematically observed on faults that have just ruptured, though such faults have suddenly been relaxed from tectonic stress. That such a zone of stress decrease can be characterized by vigorous triggering is at odds with a simple mechanical model that would relate area-averaged stress changes with area-averaged seismicity changes. We have investigated here whether the small-scale variability of stress change that cannot be deterministically modeled, can explain such an observation. Realistic values of on-fault stress randomness, caused by the coseismic slip heterogeneity are effectively seen to promote aftershock triggering. This is a clear indication that other, i.e., off-fault, instances of noncorrelation between stress decrease and seismicity rate drop (at the scale of days to months), as observed by *Parsons* [2002], *Marsan* [2003], and *Felzer and Brodsky* [2005], could also be related to small-scale stress variability.

[39] A model based on rate-and-state friction was used to relate stress to seismicity rates. Such a model predicts that the total number (i.e., over a very long time) of earthquakes triggered by a distribution of stress change is proportional to the mean of this distribution, though it is strongly sensitive to its variance at short timescales. On-fault seismicity is therefore expected to eventually drop at such long timescales, following an initial triggering phase that can last from minutes to months/years, depending on the degree of stress heterogeneity.

[40] Stress variability, which can imply a mix of positive and negative stress changes over a given crustal volume much bigger than typical earthquake nucleation lengths, can also be significant off-fault, as for example due to the variability in fault geometries within this volume. The more diverse the local fault geometries are, the more likely it is to observe initial triggering in zones that are thought otherwise to be unloaded for an average fault geometry. This contrasts with Coulomb stress calculations, for which the stress tensor is projected onto one (single) specific fault geometry, for example thought to be the most representative of the local tectonics [e.g., *Steacy et al.*, 2005]. Accounting for the scatter in geometry is thus likely to significantly change Coulomb stress and expected aftershock rate maps, at least at short timescales at which this variability plays an important role: complexity in the local tectonic setting can therefore enhance the disappearance of seismic shadows at the timescales of days to months. Specific case studies are here needed to estimate what can be expected as typical durations for such early triggering phases. This is an alternative mechanism to dynamical triggering for explaining both the absence of early seismic shadows, as documented by *Marsan* [2003] and *Ma et al.* [2005], or equivalently the existence of triggered earthquakes in unloaded regions [*Parsons*, 2002].

[41] More generally, any source of disorder (slip, fault geometry and roughness, the presence of damage zones in the vicinity of faults, crustal small-scale heterogeneity like changes in lithology or in elastic properties, further roughening of the stress field caused by aftershock occurrences (which add significant stress at sites of pending aftershocks [see *Marsan*, 2005]), variability in pore fluid pressure and its dynamics (controlled by the heterogeneous crustal permeability), etc.) is expected to promote initial triggering in zones that are otherwise unloaded on average. Slip variability is thought to be the strongest source of disorder, responsible for the intense on-fault triggering, but other sources may have a significant control on off-fault seismicity.

[42] For a stress change decaying with the distance r from the fault in r^{-3}, and assuming that the stress variability decays roughly the same, the condition $\sigma_\tau > \sqrt{2|\overline{\tau}|}$ (see section 2.2) for the existence of an initial triggering period cannot be met at large distances, though it clearly can at shorter ones. So there must exist some characteristic distance from the fault, within which no quiescence can be seen immediately after the main shock. Such an immediate quiescence is only likely to be seen far enough from the main fault, though the difficulty of statistically detecting it at too short a timescale (see *Marsan and Nalbant* [2005] for a detailed discussion on this issue) and the possible existence of early dynamic triggering can imply that seismicity analyses hardly find any.

[43] As an example, the change in right-lateral shear stress is computed, following the occurrence of a 10 km $\times$ 10 km earthquake on a vertical plane, with the fine-scale slip distribution shown in Figure 6. This slip is resolved at the 40 m scale, and is generated by a k^{-1-H} model with $H = 0.7$ tapered at the edges. It has a mean of 1 m, reaches a maximum of about 2.6 m, and corresponds to pure strike-slip motion. The stress change is computed with a boundary element code [*Gomberg and Ellis*, 1994] that uses the dislocation solution of *Okada* [1992] for the displacement and deformation. The stress is resolved at the 60 m scale, on vertical planes parallel to the main fault plane located at various distances (0, 100 m, 200 m, 500 m, 1 km, 5 km) from it (see Figure 7). The variability of the stress field decays quickly with distance, but the mean change in shear stress remains negative at all those distances. The changes

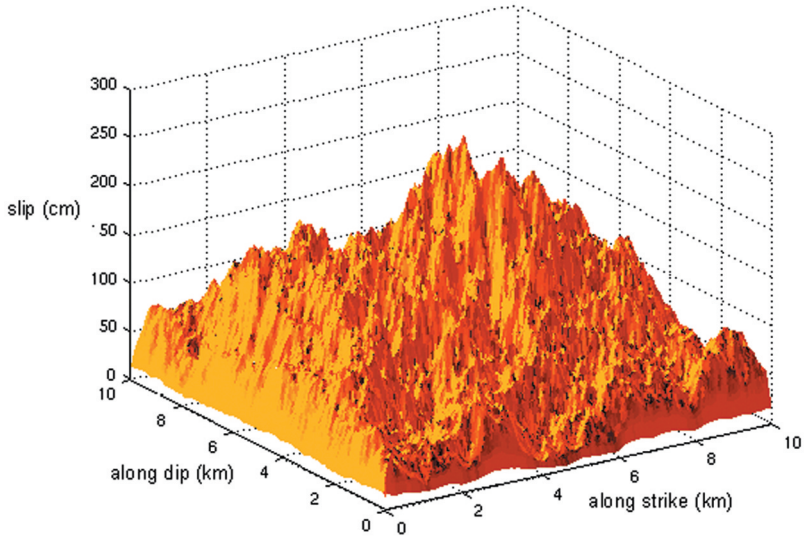


Figure 6. Slip distribution at the 40 m scale generated by a $k^{-1.7}$ model tapered at the edges, for a 10 km $\times$ 10 km pure strike-slip earthquake.

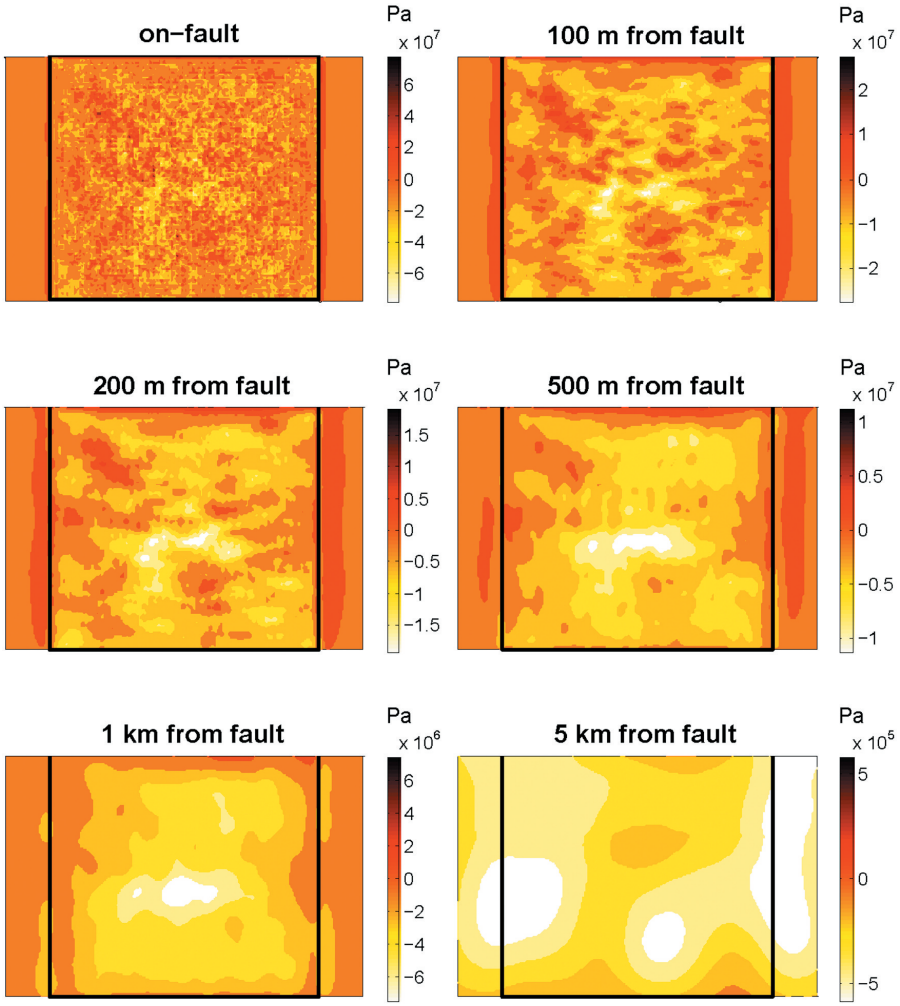


Figure 7. Changes in shear stress resolved at the 60 m scale, for vertical planes parallel to the main fault plane of Figure 6, at various distances from it. The projection of the 10 km $\times$ 10 km main fault is shown with a box. Vertical coordinate is updip.

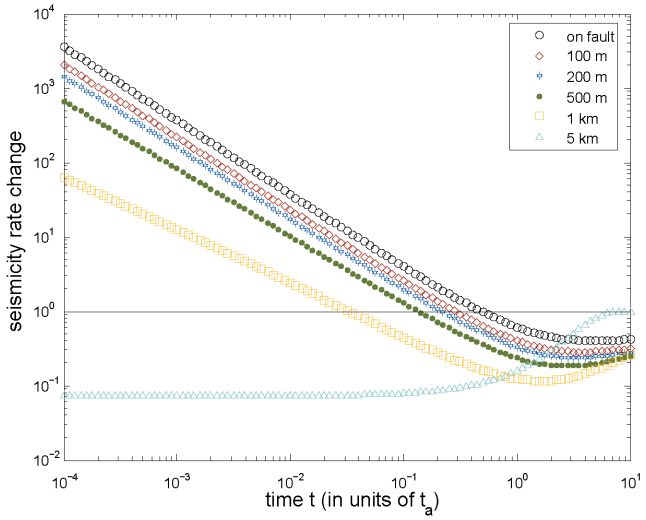


Figure 8. Changes in seismicity rates for the six planes of Figure 7 limited to the projected main fault plane (boxes of Figure 7). These rates are computed taking $A\sigma = 0.1$ MPa. All planes experience initial triggering, apart from the one at 5 km. Quiescence follows in all cases.

in seismicity rates are computed assuming $A\sigma = 0.1$ MPa and a mean friction coefficient of $\mu = 0.4$ (compare Figure 8). Only the plane at 5 km experiences an immediate quiescence, while it is delayed for the other planes closer to the main fault plane.

[44] As observed on Figure 7, stress variability due to the complex fine-scale-slip distribution decays quickly away from the fault. Other sources of noise can then become important. To illustrate this, a 50% stress variability was added to the Coulomb stress resolved at the 100 m scale, shown on Figure 9 at the 5 km depth: the Coulomb stress change in any 100 m $\times$ 100 m cell is randomly variable according to a Gaussian distribution, centered on the actual stress value as given by the boundary element code, and with a 50% standard deviation. Seismicity rate changes were then calculated based on equation (6) at $t = 10^{-3}$, 0.1 and 10 times t_a, for $A\sigma = 0.1$ MPa. Very strong triggering is observed at $t = 10^{-3}$ on-fault and within the coseismic zone. This triggering then decays with time in $1/t$, but is still active at $t = 0.1$ over most of the rupture zone. Quiescence is already observed at $t = 10^{-3}$ far away from the fault, to further spread at $t = 10$ although with a change in seismicity rate ranging between 0.5 and 1 only. While most of the modeled 30 km $\times$30 km region was primarily unloaded by the earthquake, the stress variability has clearly suppressed the quiescence at timescales less than about 1.

[45] Seismicity shadows are therefore expected to be found early in aftershock sequences only in areas of stress release characterized by little stress disorder. Faults with large cumulative offsets [*Jones*, 1997], very simple geometrical structures, and little off-fault seismicity, as with creeping faults in northern California, are possible candidates. Indeed, relatively clear quiescences have been observed in the first 100 days following the 1989 Loma Prieta earthquake along such faults, and most notably the Hayward and Calaveras faults [*Marsan*, 2003]. This strongly contrasts with what was observed in southern California after the 1992 Landers and 1994 Northridge earthquakes. Also, the

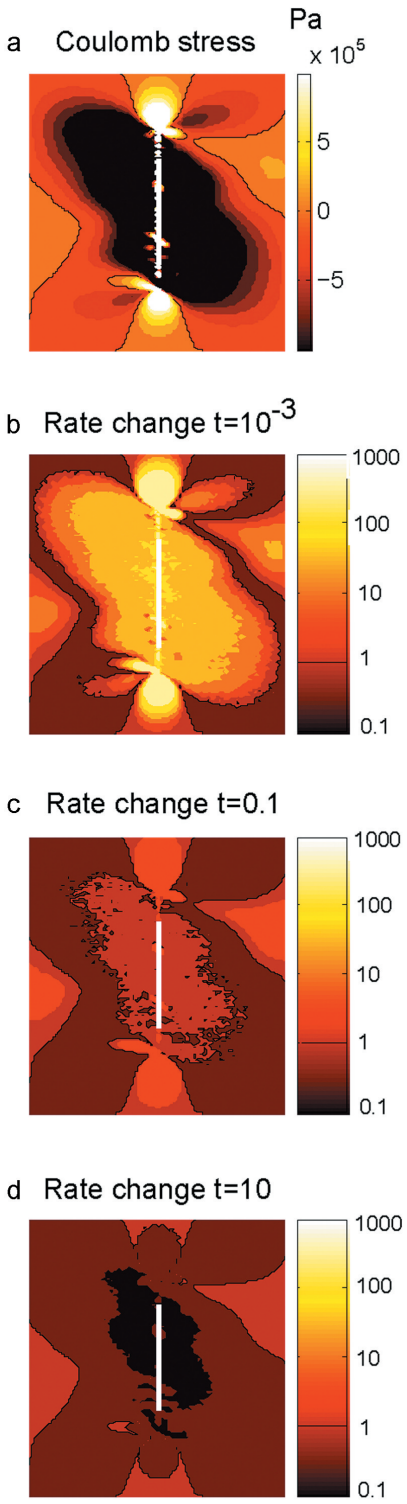


Figure 9. Coulomb stress and seismicity changes for the 10 km long vertical strike-slip fault of Figure 6, for a 30 km long region. (a) Coulomb stress change for a friction coefficient of 0.4, at 5 km depth, seen at a 100 m resolution. The zero contour is shown in black. (b–d) Seismicity rate changes at the 5 km depth, at $t = 10^{-3}$, 0.1, and 10 (in units of t_a), calculated from the Coulomb stress change to which variability was added, see text. The contour in black separates the triggered from the quiescent areas.

great 1857 Fort Tejon and 1906 San Francisco earthquakes are believed to have been relatively little productive in terms of aftershock triggering, a phenomenon that could be related to the large cumulative offsets on the San Andreas fault [*Meltzner and Wald*, 2003]. Interestingly, these authors also note that the decay of these two aftershock sequences seems to have been slow, which is consistent with the results of section 2.2 (Figure 1) where little disorder implied little active and slow decaying triggering phases (see also Helmstetter and Shaw, submitted manuscript, 2005).

[46] Finally, smooth aseismic slip can be thought of as creating less heterogeneous a stress field than the rapid, inertially controlled seismic rupture. A clear instance of a sudden seismicity rate decrease has been reported to occur at shallow depth about 6 months after the Landers earthquake, east of the rupture [*Ogata et al.*, 2003; see also *Marsan and Nalbant*, 2005]. Other cases of quiescences with relatively sharp onsets are documented by *Ogata* [1992, 2005], occurring before large earthquakes. Such observations have prompted to propose that aseismic slip, perhaps precursory to such earthquakes (and to the Hector Mine earthquake in the case of the Landers sequence [see *Ogata et al.*, 2003]), can create observable shadows.

[47] **Acknowledgments.** I would like to thank Clifford Thurber, Karen Felzer, and Tom Parsons for constructive reviews and my colleagues from the Fluids and Dynamics of the Lithosphere research group at the LGIT for inspiring discussions. This paper was written while visiting the Department of Geology at the University College Dublin, thanks to an Egide grant (Ulysses).

References

Abercrombie, R., and P. Leary (1993), Source parameters of small earthquakes recorded at 2.5 km depth, Cajon Pass, southern California: Implications for earthquake scaling, *Geophys. Res. Lett.*, *20*(14), 1511–1514.

Andrews, D. J. (1980), A stochastic fault model: 1. Static case, *J. Geophys. Res.*, *85*, 3867–3877.

Belardinelli, M. E., A. Bizzarri, and M. Cocco (2003), Earthquake triggering by static and dynamic stress changes, *J. Geophys. Res.*, *108*(B3), 2135, doi:10.1029/2002JB001779.

Beroza, G. C., and W. L. Ellsworth (1996), Properties of the seismic nucleation phase, *Tectonophysics*, *261*, 209–227.

Bouchon, M. (1997), The state of stress on some faults of the San Andreas system as inferred from near-field strong motion data, *J. Geophys. Res.*, *102*, 11,731–11,744.

Bouchon, M., H. Sekiguchi, K. Irikura, and T. Iwata (1998), Some characteristics of the stress field of the 1995 Hyogo-ken Nanbu (Kobe) earthquake, *J. Geophys. Res.*, *103*, 24,271–24,282.

Dalguer, L. A., K. Irikura, W. Zhang, and J. D. Riera (2002), Distribution of dynamic and static stress changes during 2000 Tottori (Japan) earthquake: Brief interpretation of the earthquake sequences: Foreshocks, mainshock and aftershocks, *Geophys. Res. Lett.*, *29*(16), 1758, doi:10.1029/2001GL014333.

Daniel, G., D. Marsan, and M. Bouchon (2006), Perturbation of the Izmit earthquake aftershock decaying activity following the 1999 M_w 7.2 Dzce, Turkey, earthquake, *J. Geophys. Res.*, *111*, B05310, doi:10.1029/2005JB003978.

Day, S. M., G. Yu, and D. J. Wald (1998), Dynamic stress changes during earthquake rupture, *Bull. Seismol. Soc. Am.*, *88*(2), 512–522.

Dieterich, J. H. (1979), Modeling of rock friction: 1. Experimental results and constitutive equations, *J. Geophys. Res.*, *84*, 2161–2168.

Dieterich, J. H. (1986), A model for the nucleation of earthquake slip, in *Earthquake source mechanics*, *Geophys. Monogr. Ser.* , vol. 37, edited by S. Das, J. Boatwright, and C. H. Scholz, pp. 37–47, AGU, Washington, D. C.

Dieterich, J. H. (1994), A constitutive law for rate of earthquake production and its application to earthquake clustering, *J. Geophys. Res.*, *99*, 2601–2618.

Dieterich, J. H. (1995), Earthquake simulations with time-dependent nucleation and long-range interaction, *Nonlinear Process. Geophys.*, *2*, 109–120.

Dodge, D. A., G. C. Beroza, and W. L. Ellsworth (1995), Detailed observations of California foreshock sequences: Implications for the earthquake initiation process, *J. Geophys. Res.*, *101*, 22,371–22,392.

Ellsworth, W. L., A. G. Lindh, W. H. Prescott, and D. G. Herd (1981), The 1906 San Francisco earthquake ad the seismic cycle, in *Earthquake Prediction: An International Review*, *Maurice Edwing Ser.*, vol. 4, edited by D. W. Simpson and P. G. Richards, AGU, Washington, D. C.

Felzer, K. R., and E. E. Brodsky (2005), Testing the stress shadow hypothesis, *J. Geophys. Res.*, *110*, B05S09, doi:10.1029/2004JB003277.

Felzer, K. R., T. W. Becker, R. E. Abercrombie, G. Ekström, and J. R. Rice (2002), Triggering of the 1999 M_w 7.1 Hector Mine earthquake by aftershocks of the 1992 M_w 7.3 Landers earthquake, *J. Geophys. Res.*, *107*(B9), 2190, doi:10.1029/2001JB000911.

Felzer, K. R., R. E. Abercrombie, and G. Ekström (2004), A common origin for aftershocks, foreshocks, and multiplets, *Bull. Seismol. Soc. Am.*, *94*(1), 88–98.

Fischer, T., and J. Horálek (2005), Slip-generated patterns of swarm microearthquakes from West Bohemia/Vogtland (central Europe): Evidence of their triggering mechanism?, *J. Geophys. Res.*, *110*, B05S21, doi:10.1029/2004JB003363.

Frankel, A. (1991), High-frequency spectral fallof of earthquakes, fractal dimension of complex rupture, *b* value, and the scaling of strength on fault, *J. Geophys. Res.*, *96*, 6291–6302.

Gomberg, J., and M. Ellis (1994), Topography and tectonics of the central New Madrid seismic zone: Results of numerical experiments using a three-dimensional boundary element program, *J. Geophys. Res.*, *99*, 20,299–20,310.

Gomberg, J., N. M. Beeler, M. L. Blanpied, and P. Bodin (1998), Earthquake triggering by transient and static deformations, *J. Geophys. Res.*, *103*, 24,411–24,426.

Gomberg, J., P. Bodin, and P. A. Reasenberg (2003), Observing earthquakes triggered in the near field by dynamic deformations, *Bull. Seismol. Soc. Am.*, *93*(1), 118–138.

Gomberg, J., P. Reasenberg, M. Cocco, and M. E. Belardinelli (2005), A frictional population model of seismicity rate change, *J. Geophys. Res.*, *110*, B05S03, doi:10.1029/2004JB003404.

Hanks, T. C. (1977), Earthquake stress drops, ambient tectonic stresses, and stresses that drive plates, *Pure Appl. Geophys.*, *115*, 441–458.

Harris, R. A., and R. W. Simpson (1996), In the shadow of 1857: The effect of the great Ft. Tejon earthquake on subsequent earthquakes in southern California, *Geophys. Res. Lett.*, *23*(3), 229–232.

Harris, R. A., and R. W. Simpson (1998), Suppression of large earthquakes by stress shadows: A comparison of Coulomb and rate-and-state failure, *J. Geophys. Res.*, *103*, 24,439–24,451.

Helmstetter, A. (2003), Is earthquake triggering driven by small earthquakes?, *Phys. Rev. Lett.*, *91*(5), 058501.

Helmstetter, A., Y. Y. Kagan, and D. D. Jackson (2005), Importance of small earthquakes for stress transfers and earthquake triggering, *J. Geophys. Res.*, *110*, B05S08, doi:10.1029/2004JB003286.

Herrero, A., and P. Bernard (1994), A kinematic self-similar rupture process for earthquakes, *Bull. Seismol. Soc. Am.*, *84*(4), 1216–1288.

Jones, L. M. (1997), Aftershock productivity as a function of cumulative fault offsets, *Seismol. Res. Lett.*, *68*, 331.

Kilb, D., J. Gomberg, and P. Bodin (2000), Triggering of earthquake aftershocks by dynamic stresses, *Nature*, *408*(6812), 570–574.

Kilb, D., J. Gomberg, and P. Bodin (2002), Aftershock triggering by complete Coulomb stress changes, *J. Geophys. Res.*, *107*(B4), 2060, doi:10.1029/2001JB000202.

Lapusta, N., and J. R. Rice (2003), Nucleation and early seismic propagation of small and large events in a crustal earthquake model, *J. Geophys. Res.*, *108*(B4), 2205, doi:10.1029/2001JB000793.

Lavallée, D., and R. J. Archuleta (2003), Stochastic modeling of slip spatial complexities for the 1979 Imperial Valley, California, earthquake, *Geophys. Res. Lett.*, *30*(5), 1245, doi:10.1029/2002GL015839.

Lavallée, D., and R. J. Archuleta (2005), Coupling of the random properties of the source and the ground motion for the 1999 Chi Chi earthquake, *Geophys. Res. Lett.*, *32*, L08311, doi:10.1029/2004GL022202.

Ma, K., C. Chan, and R. S. Stein (2005), Response of seismicity to Coulomb stress triggers and shadows of the 1999 M_w = 7.6 Chi-Chi, Taiwan, earthquake, *J. Geophys. Res.*, *110*, B05S19, doi:10.1029/2004JB003389.

Mai, P. M., and G. C. Beroza (2002), A spatial random field model to characterize complexity in earthquake slip, *J. Geophys. Res.*, *107*(B11), 2308, doi:10.1029/2001JB000588.

Marsan, D. (2003), Triggering of seismicity at short timescales following Californian earthquakes, *J. Geophys. Res.*, *108*(B5), 2266, doi:10.1029/2002JB001946.

Marsan, D. (2005), The role of small earthquakes in redistributing crustal elastic stress, *Geophys. J. Int.*, *163*, 141–151.

Marsan, D., and S. S. Nalbant (2005), Methods for measuring seismicity rate changes: A review and a study of how the M_w 7.3 Landers earth-

quake affected the aftershock sequence of the M_w 6.1 Joshua Tree earthquake, *Pure Appl. Geophys.*, *162*(6–7), 1151–1185.

Meltzner, A. J., and D. J. Wald (1999), Foreshocks and aftershocks of the great 1857 California earthquake, *Bull. Seismol. Soc. Am.*, *89*(4), 1109–1120.

Meltzner, A. J., and D. J. Wald (2003), Aftershocks and triggered events of the Great 1906 California earthquake, *Bull. Seismol. Soc. Am.*, *93*(5), 2160–2186.

Mikumo, T., and T. Miyatake (1995), Heterogeneous distribution of dynamic stress drop and relative fault strength recovered from the resultrs of wave-form inversion—The 1984 Morgan-Hill, California, earthquake, *Bull. Seismol. Soc. Am.*, *85*(1), 178–193.

Ogata, Y. (1992), Detection of precursory relative quiescence before great earthquakes through a statistical model, *J. Geophys. Res.*, *97*, 19,845–19,871.

Ogata, Y. (2005), Detection of anomalous seismicity as a stress change sensor, *J. Geophys. Res.*, *110*, B05S06, doi:10.1029/2004JB003245.

Ogata, Y., L. M. Jones, and S. Toda (2003), When and where the aftershock activity was depressed: Contrasting decay patterns of the proximate large earthquakes in southern California, *J. Geophys. Res.*, *108*(B6), 2318, doi:10.1029/2002JB002009.

Okada, Y. (1992), Internal deformation due to shear and tensile faults in a half-space, *Bull. Seismol. Soc. Am.*, *82*(2), 1018–1040.

Parsons, T. (2002), Global Omori law decay of triggered earthquakes: Large aftershocks outside the classical aftershock zone, *J. Geophys. Res.*, *107*(B9), 2199, doi:10.1029/2001JB000646.

Parsons, T. (2005), A hypothesis for delayed dynamic earthquake triggering, *Geophys. Res. Lett.*, *32*, L04302, doi:10.1029/2004GL021811.

Perfettini, H., and J.-P. Avouac (2004), Postseismic relaxation driven by brittle creep: A possible mechanism to reconcile geodetic measurements and the decay rate of aftershocks, application to the Chi-Chi earthquake, Taiwan, *J. Geophys. Res.*, *109*, B02304, doi:10.1029/2003JB002488.

Perfettini, H., J. Schmittbuhl, and A. Cochard (2003), Shear and normal load perturbations on a two-dimensional continuous fault: 1. Static triggering, *J. Geophys. Res.*, *108*(B9), 2408, doi:10.1029/2002JB001804.

Ripperger, J., and P. M. Mai (2004), Fast computation of static stress changes on 2D faults from final slip distributions, *Geophys. Res. Lett.*, *31*, L18610, doi:10.1029/2004GL020594.

Rubin, A. M., and D. Gillard (2000), Aftershock asymmetry/rupture directivity among central San Andreas fault microearthquakes, *J. Geophys. Res.*, *105*, 19,095–19,110.

Ruina, A. (1983), Slip instability and state variable friction laws, *J. Geophys. Res.*, *88*, 10,359–10,370.

Steacy, S., S. S. Nalbant, J. McCloskey, C. Nostro, O. Scotti, and D. Baumont (2005), Onto what planes should Coulomb stress perturbations be resolved?, *J. Geophys. Res.*, *110*, B05S15, doi:10.1029/2004JB003356.

Toda, S., R. S. Stein, P. A. Reasenberg, J. H. Dieterich, and A. Yoshida (1998), Stress transferred by the 1995 M_w = 6.9 Kobe, Japan, shock: Effect on aftershocks and future earthquake probabilities, *J. Geophys. Res.*, *103*, 24,543–24,566.

Voisin, C., M. Campillo, I. R. Ionescu, F. Cotton, and O. Scotti (2000), Dynamic versus static stress triggering and friction parameters: Inferences from the November 23, 1980, Irpinia earthquake, *J. Geophys. Res.*, *105*, 21,647–21,660.

Voisin, C., F. Cotton, and S. Di Carli (2004), A unified model for dynamic and static stress triggering of aftershocks, antishocks, remote seismicity, creep events, and multisegmented rupture, *J. Geophys. Res.*, *109*, B06304, doi:10.1029/2003JB002886.

Zhang, W., T. Iwata, K. Irikura, H. Sekiguchi, and M. Bouchon (2003), Heterogeneous distribution of the dynamic source parameters of the 1999 Chi-Chi, Taiwan, earthquake, *J. Geophys. Res.*, *108*(B5), 2232, doi:10.1029/2002JB001889.

Ziv, A., and A. M. Rubin (2003), Implications of rate-and-state friction for properties of aftershock sequence: Quasi-static inherently discrete simulations, *J. Geophys. Res.*, *108*(B1), 2051, doi:10.1029/2001JB001219.

D. Marsan, Laboratoire de Géophysique Interne et Tectonophysique, Université de Savoie, F-73376 Le Bourget du Lac, France. (david.marsan@univ-savoie.fr)